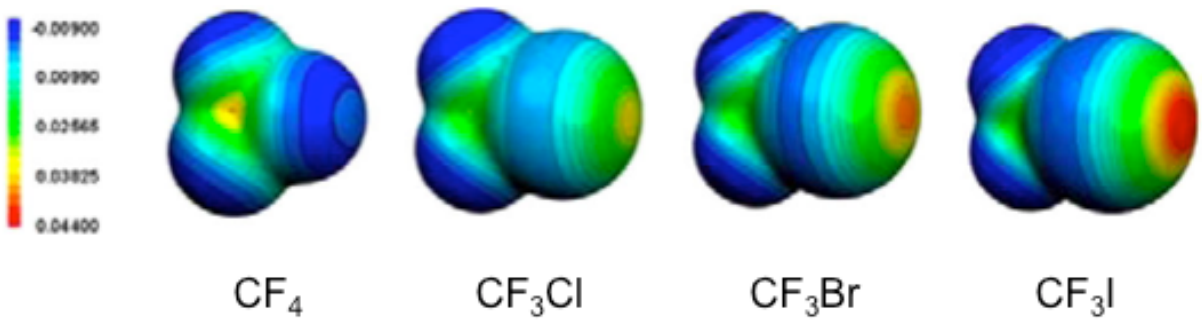

Supplementary figure 1 | Molecular electrostatic potential surface of CF_3X. Reprinted with permission from Supplementary Reference #4. Copyright 2007 Springer.

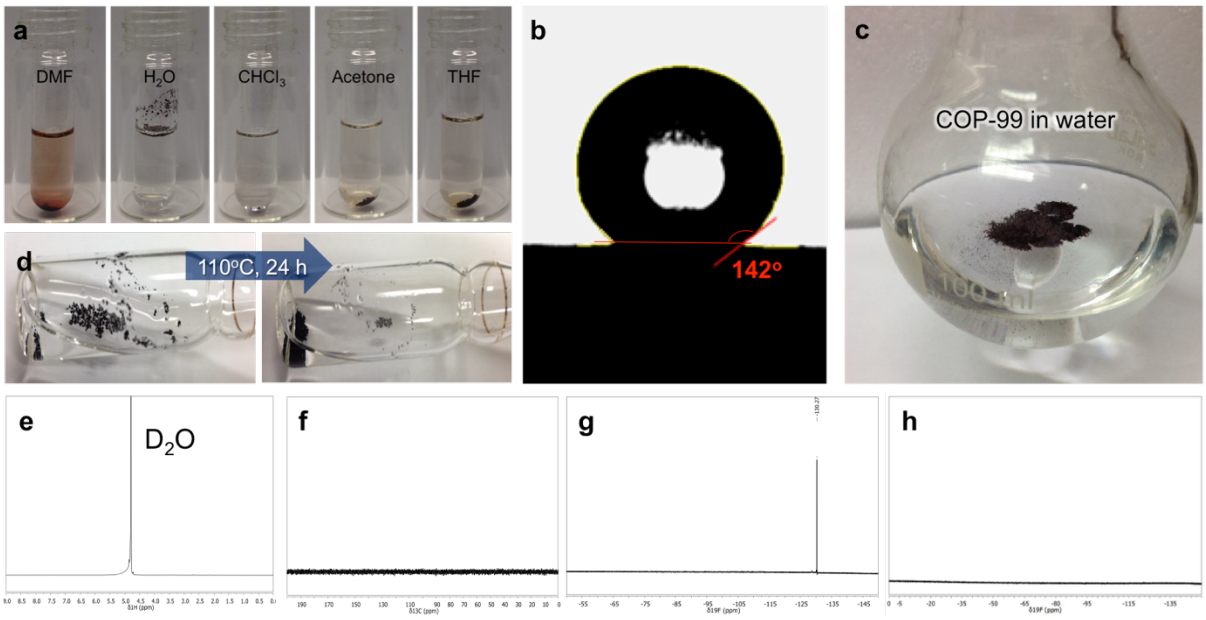

Supplementary figure 2 | Stability tests for COP-99. (**a**) Solubility test of COP-99 in common solvents. Images were taken after a sonication for 1 min at 50 °C. (**b**) Contact angle for a water droplet on the surface of COP-99. (**c**) Photograph of COP-99 in water. Owing to the hydrophobicity, COP-99 floats on the surface of water. (**d**) Long-term boiling test of COP-99 (20 mg) in D_2O (1.5 mL) at 110°C for 24 h. In order to prevent D_2O evaporation, the test was conducted in a sealed glass ampoule. There was no noticeable change in both COP-99 and D_2O solution after boiling. (**e**) ^{1}H and (**f**) ^{13}C NMR spectrum of the D_2O filtrate. (**g**) ^{19}F NMR spectrum of D_2O the filtrate exhibited the existence of free fluorine partially detached from COP-99 via nucleophilic substitution. (**h**) Fluorine peak was not observed when the COP-99 was treated in D_2O at 50 °C for 60 h.

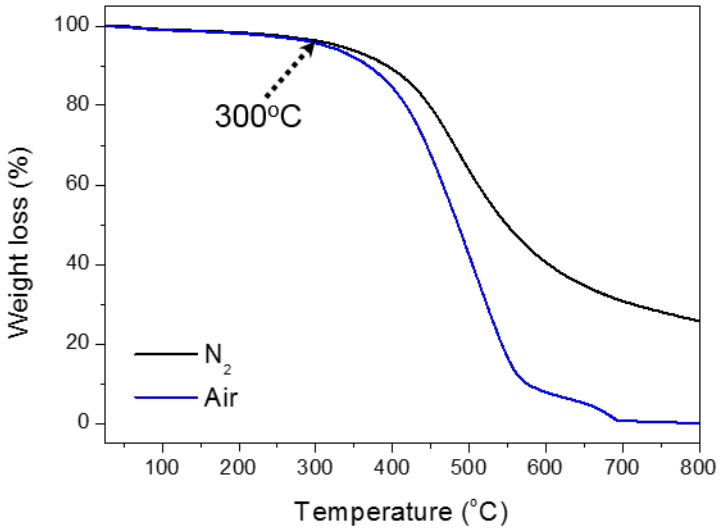

Supplementary figure 3 | Thermogravimetric analysis (TGA) plot of COP-99. COP-99 shows high thermal stability up to 300°C both in inert and oxidative environments.

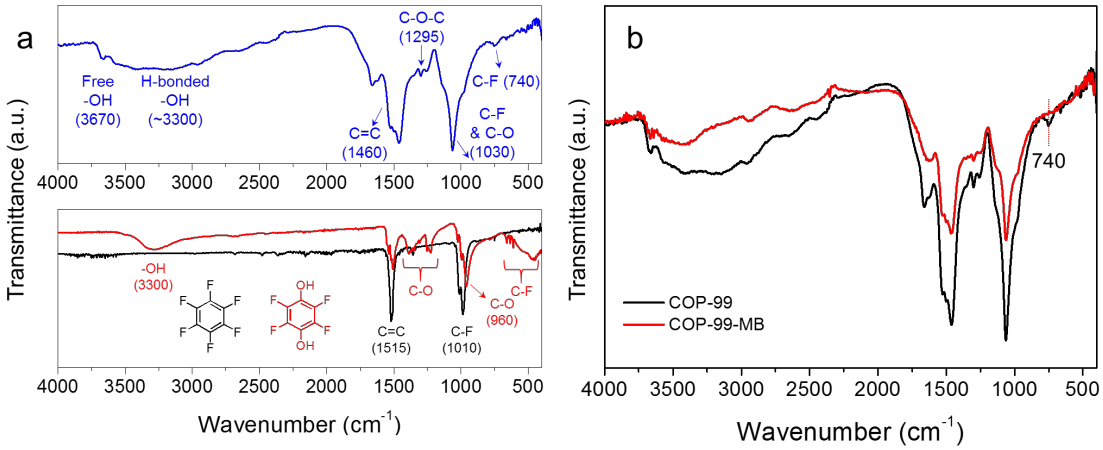

Supplementary figure 4 | Characterisation by FTIR. (**a**) FTIR spectra of COP-99 and related monomer units. (**b**) Change in FTIR spectrum after the adsorption of MB molecule.

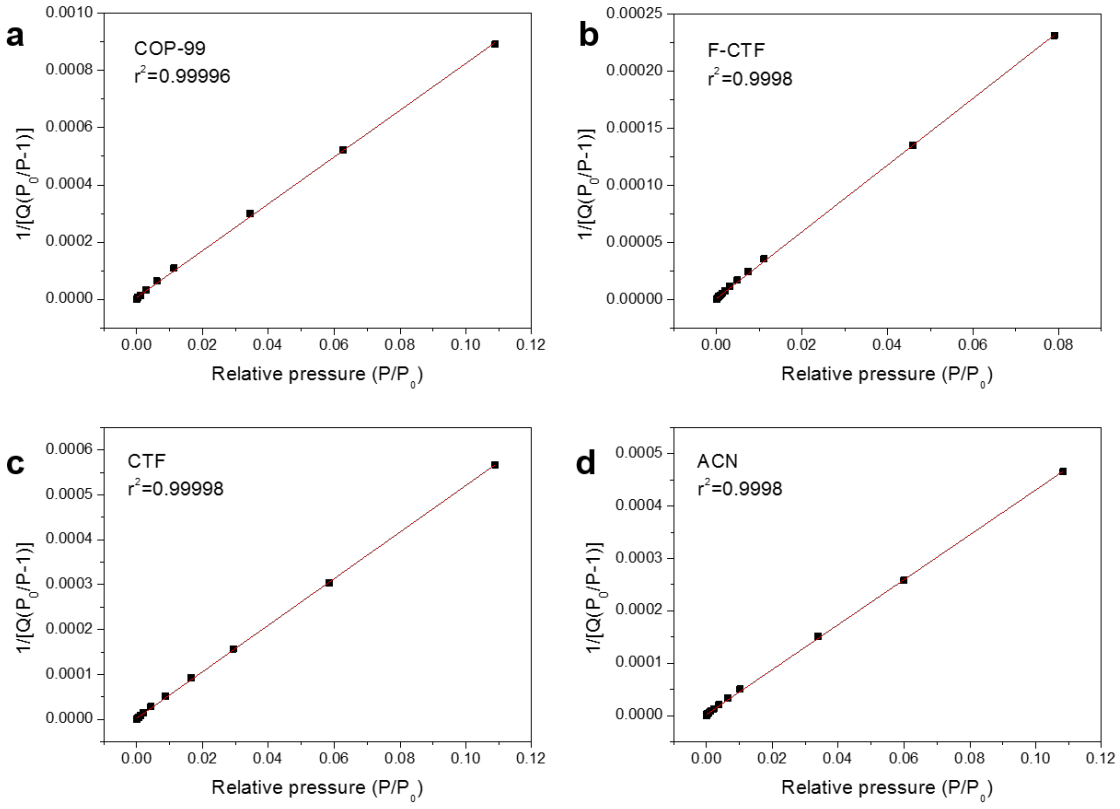

Supplementary figure 5 | BET linear plots of (**a**) COP-99, (**b**) F-CTF, (**c**) CTF, and (**d**) ACN.

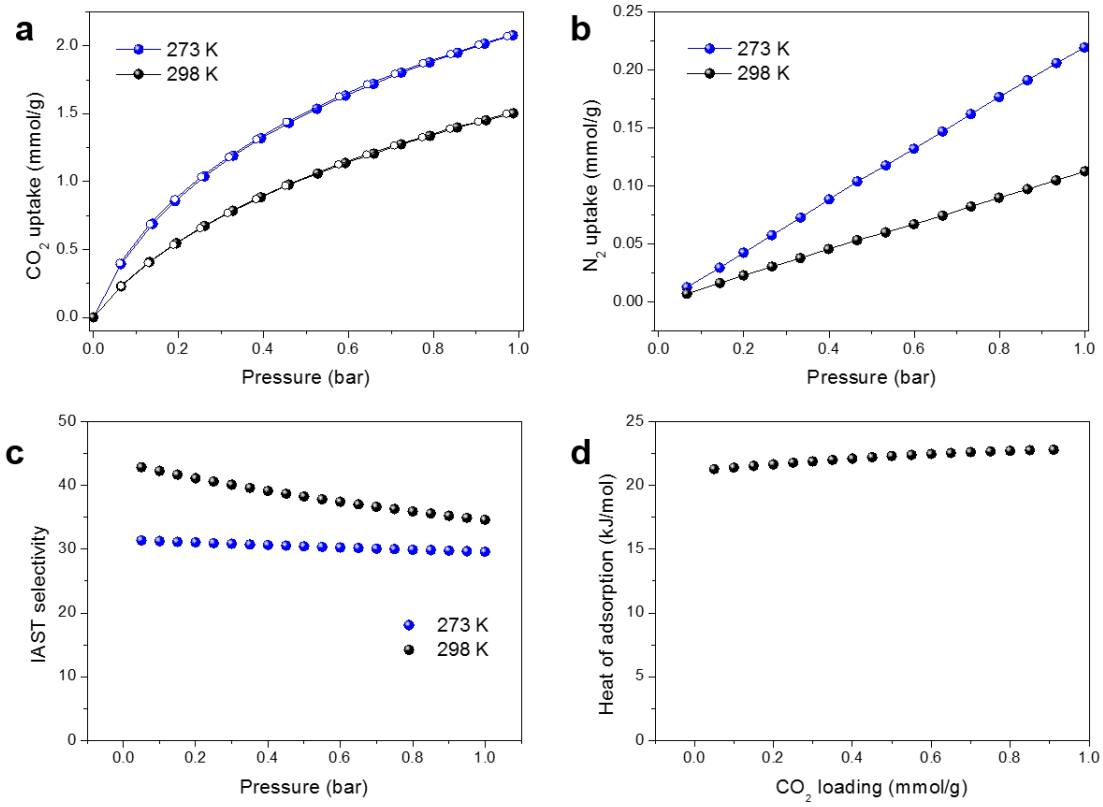

Supplementary figure 6 | Gas adsorption isotherms of COP-99; (**a**) CO_2 and (**b**) N_2 at 273 K and 298 K. (**c**) IAST CO_2/N_2 selectivity for CO_2:N_2 gas mixture (15:85). (**d**) Isosteric heat of CO_2 adsorption for COP-99.

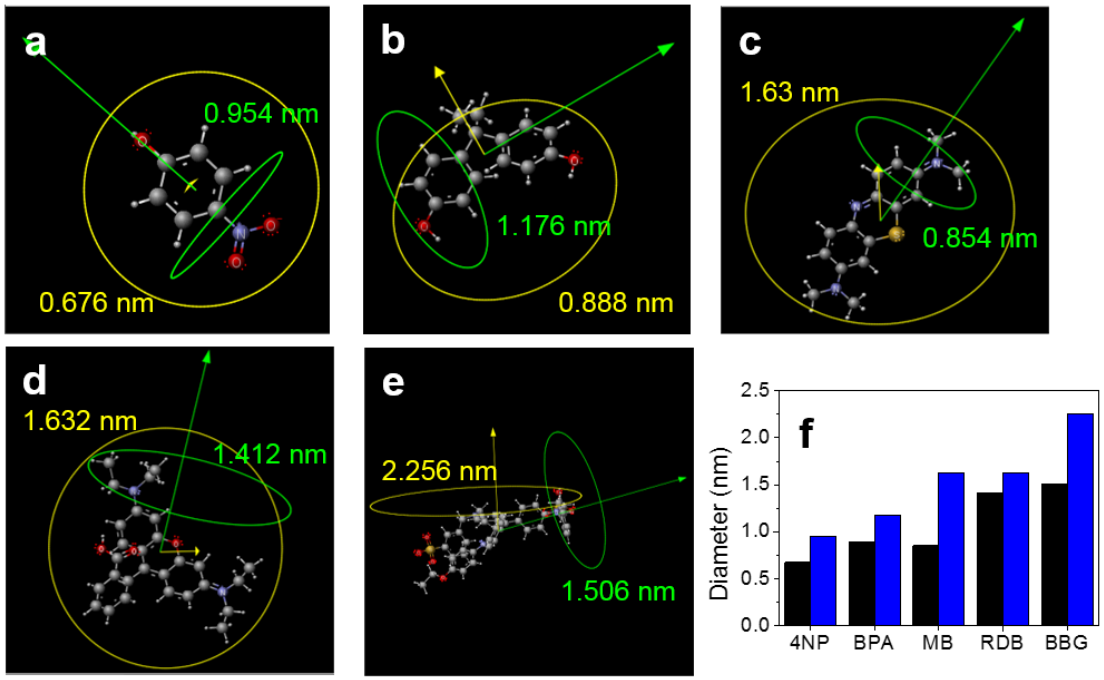

Supplementary figure 7 | Visualization of minimum (green) and maximum (yellow) projection diameter of dye molecules utilized for adsorption study; (**a**) 4-Nitrophenol (4NP), (**b**) Bisphenol A (BPA), (**c**) Methylene Blue (MB), (**d**) Rhodamine B (RDB), and (**e**) Brilliant Blue G (BBG). Arrows represent the orthogonal directions on the projection planes. (**f**) Calculated d_{min} (black) and d_{max} (blue) for dye molecules. The calculations were carried out using *MarvinSketch, ChemAxon* (version 15.6.8), for the molecular conformation with the lowest energy based on van der Waals diameter of the atoms. (Projection optimization enabled, optimization limit: very strict).

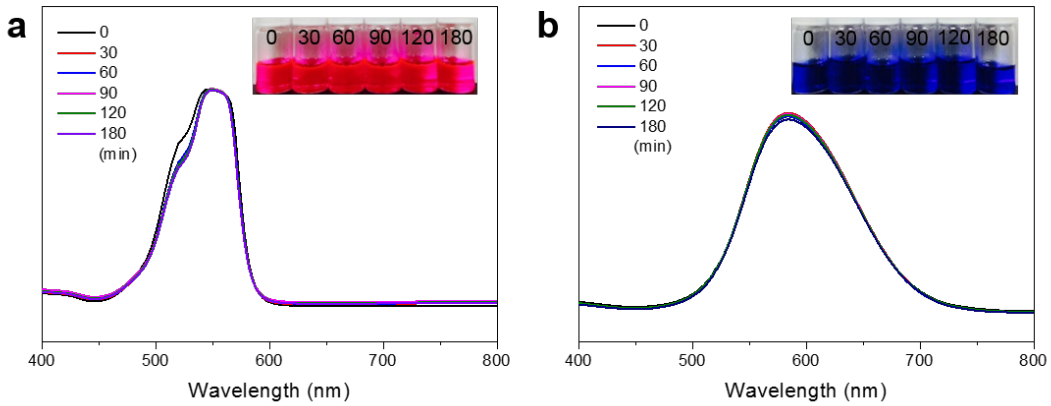

Supplementary figure 8 | UV-Vis absorption spectra of (**a**) aqueous RDB and (**b**) BBG treated with COP-99 at different intervals. The inset photograph shows the corresponding colour of the effluents after the treatment.

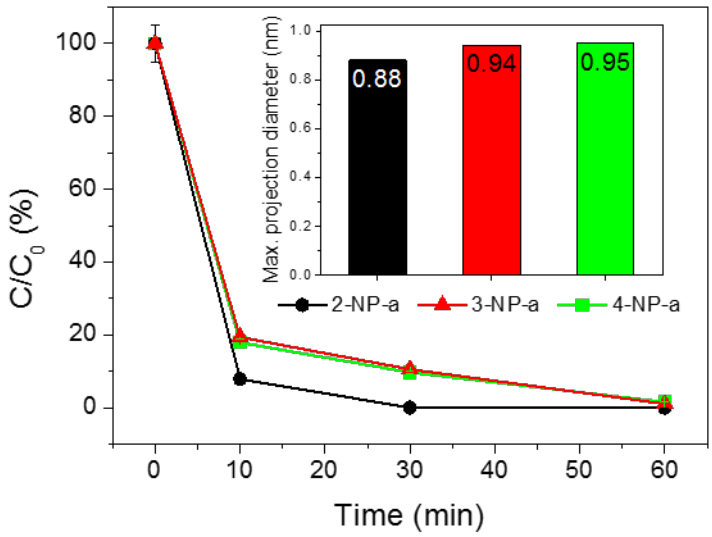

Supplementary figure 9 | Change in NP isomer concentrations over time after being treated with COP-99 in terms of absorbance relative to initial absorbance (C/C_0). Initial concentration (C_0) of all the dyes was adjusted to be 100 μM, and the adsorption was conducted in mild acid condition (pH ~3.8). Inset displays the maximum van der Waals diameter of NP isomers calculated by *MarvinSketch*.

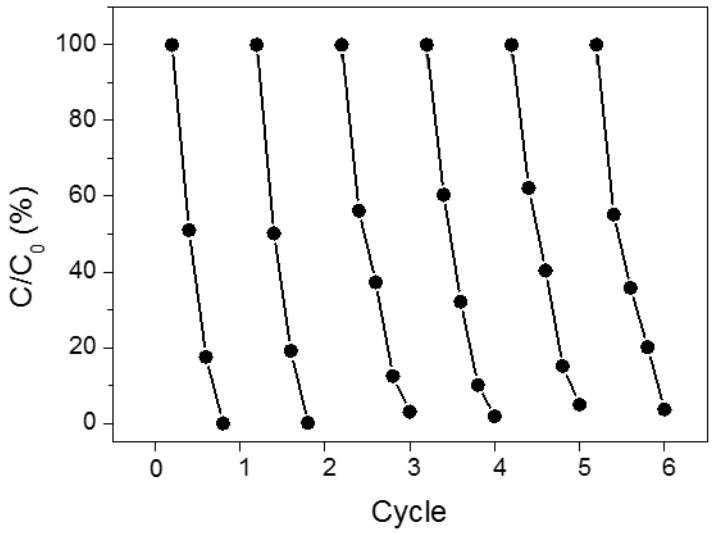

Supplementary figure 10 | Removal efficiency of 4-NP-a on COP-99 in six successive cycles of adsorption-desorption. Initial concentration of 4-NP-a was adjusted to be 50 μM and pH of all the samples was controlled to be 4.

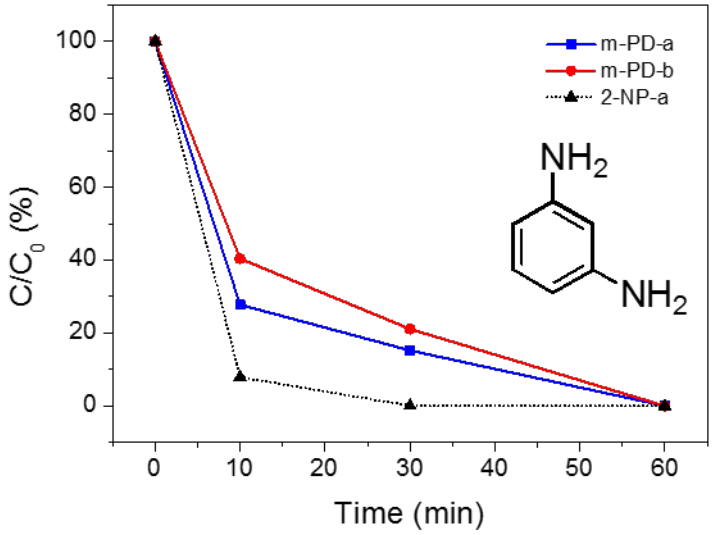

Supplementary figure 11 | Change in m-PD concentrations over time after being treated with COP-99 in terms of absorbance relative to initial absorbance (C/C_0). Initial concentration (C_0) of all the dyes was adjusted to be 100 μM. The m-PD was tested both in acidic (m-PD-a, pH = 4) and basic (m-PD-b, pH = 10) conditions. The concentration was analysed using a UV-vis spectrophotometer at a wavelength of maximum absorbance (270 nm for m-PD-a and 220 nm for m-PD-b) [10]. *Inset* shows molecular structure of m-PD.

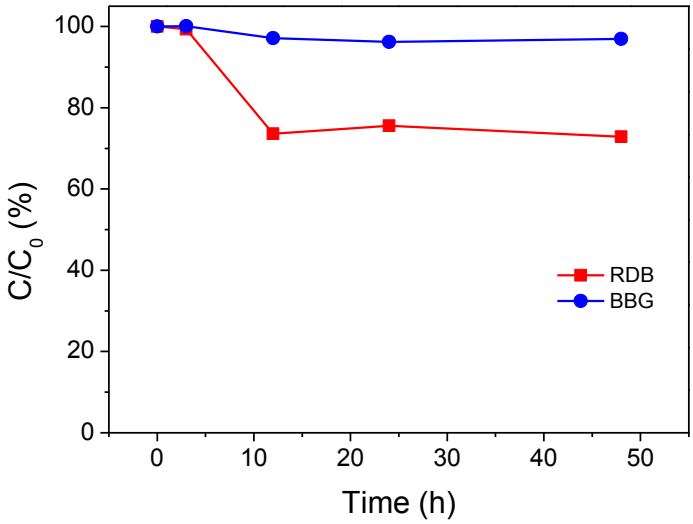

Supplementary figure 12 | Long-term adsorption test of RDB and BBG using COP-99. Initial concentration (C_0) of all the dyes was adjusted to be 50 μM.

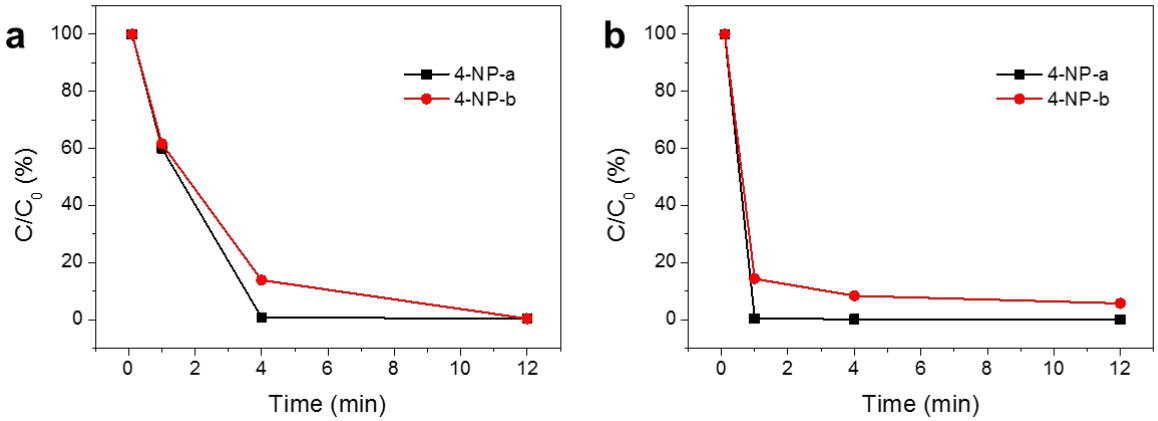

Supplementary figure 13 | Change in 4-NP concentrations over time after being treated with (**a**) CTF and (**b**) F-CTF in terms of absorbance relative to initial absorbance (C/C_0). Initial concentration (C_0) of the dyes was adjusted to be 50 μM. 4-Nitrophenol was tested both in acidic (4NP-a, pH = 4) and basic (4NP-b, pH = 9) conditions.

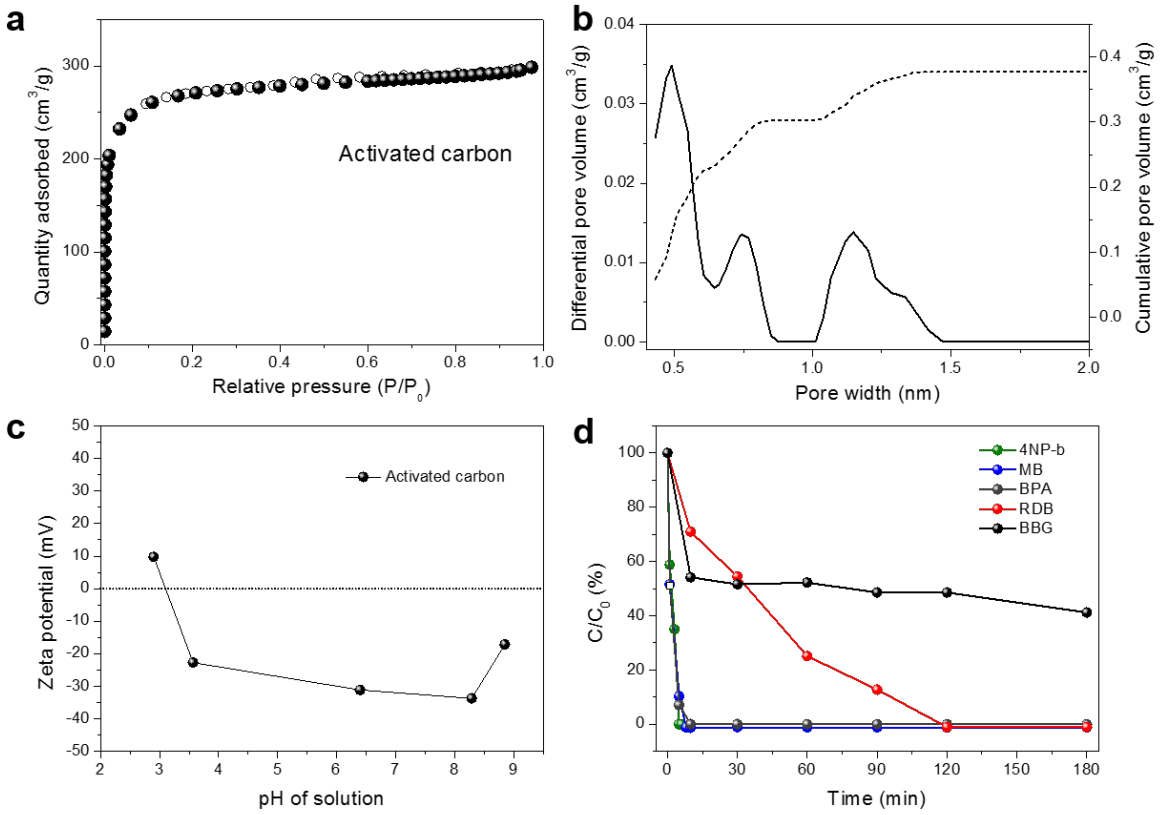

Supplementary figure 14 | Control experiments with activated carbon. (**a**) Argon adsorption-desorption isotherm of Activated Charcoal Norit® (ACN) measured at 87 K, and (**b**) corresponding NLDFT pore size distribution. (**c**) pH-dependent zeta potential of ACN. (**d**) Change in dye concentrations over time after being treated with ACN in terms of absorbance relative to initial absorbance (C/C_0). Initial concentration (C_0) of all the dyes was adjusted to be 50 μM.

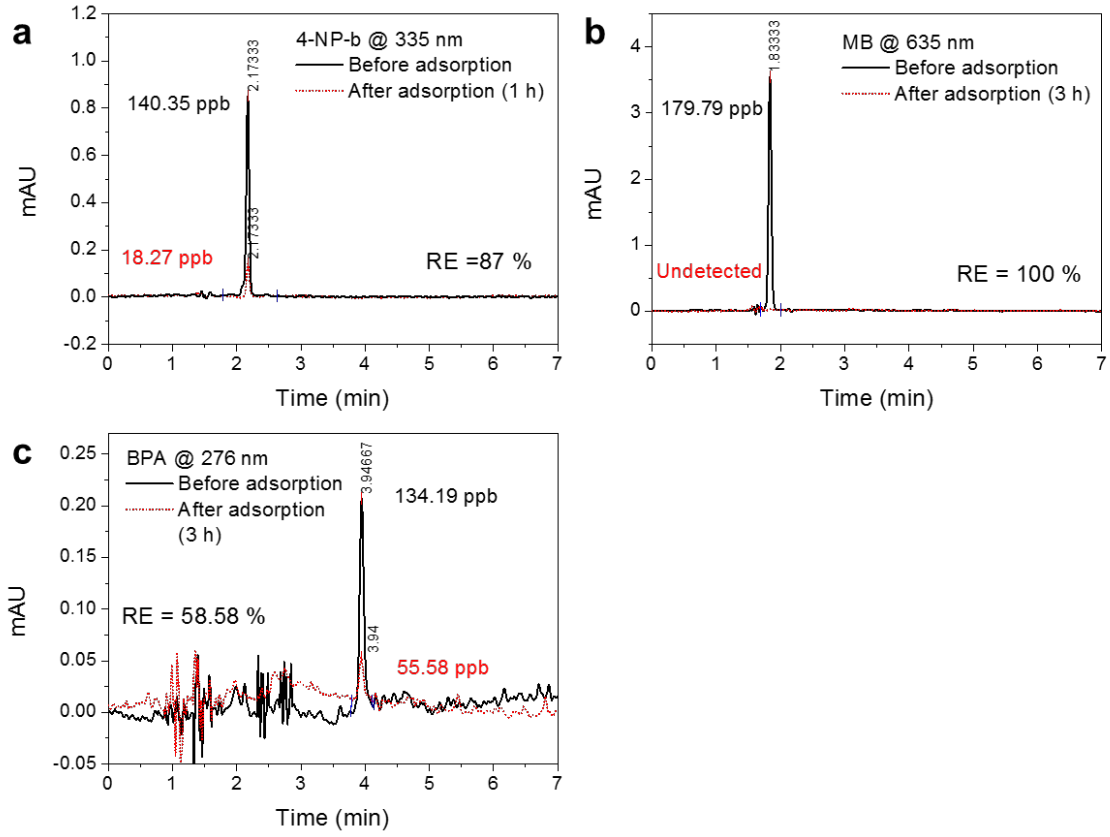

Supplementary figure 15 | LC spectra of (**a**) 4-NP-b, (**b**) MB and (**c**) BPA before and after the treatment with COP-99. RE stands for removal efficiency via the adsorption with COP-99.

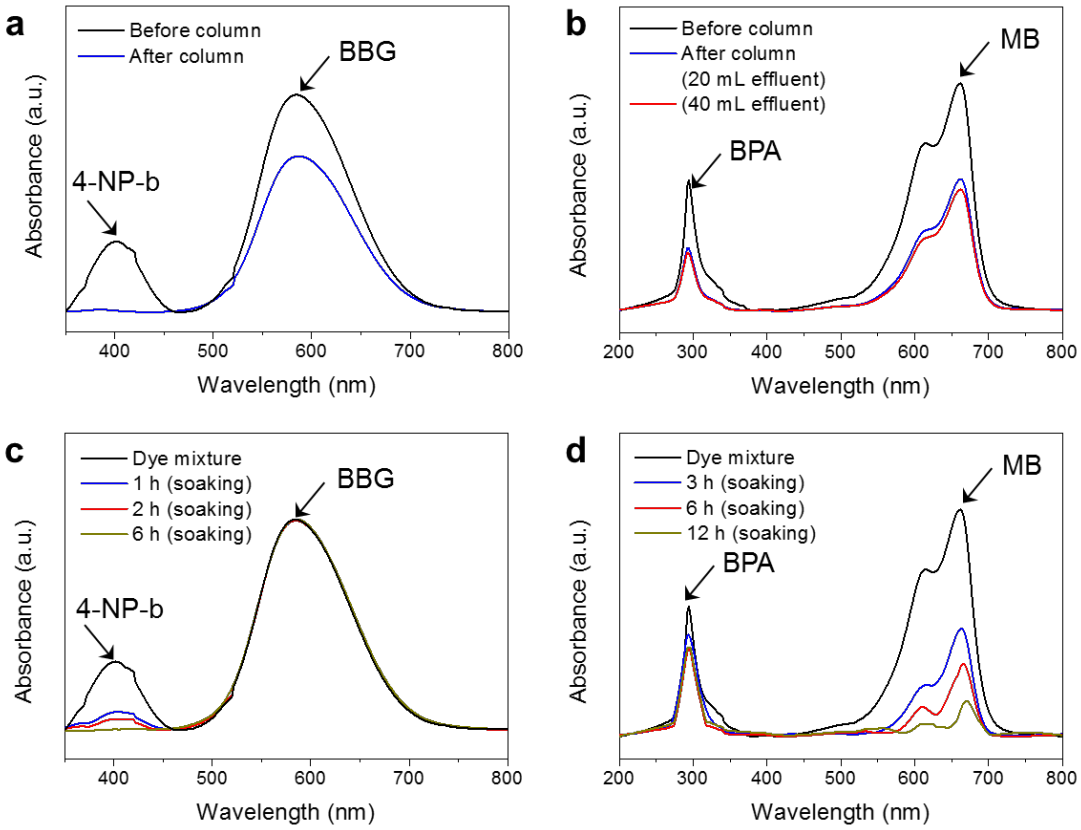

Supplementary figure 16 | UV-Vis spectra of mixed dye solutions of (**a,c**) 4-NP/BBG and (**b,d**) MB/BPA (**a, b**) before and after being treated via a packed column of COP-99 and (**c, d**) during soaking COP-99 in the solutions.

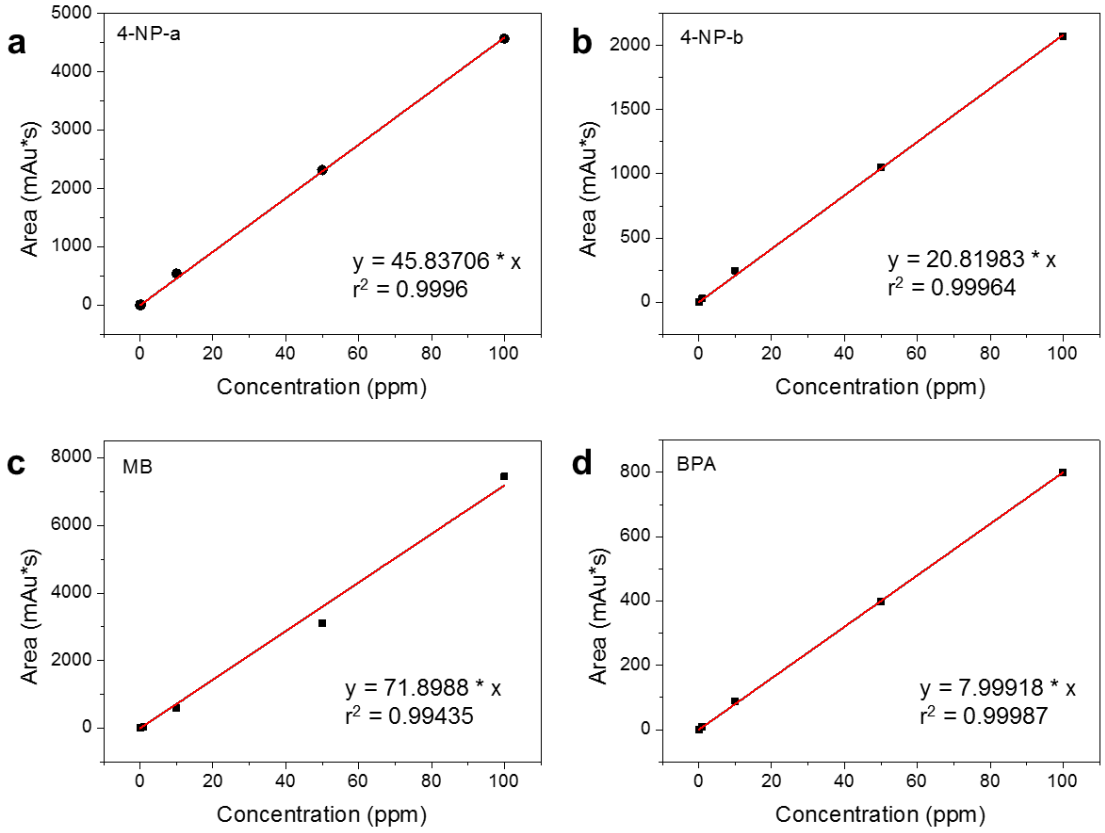

Supplementary figure 17 | HPLC calibration curves of the tested dye substrates from five concentrations of 0.05 ppm, 0.1 ppm, 10 ppm, 50 ppm, and 100 ppm. (**a**) 4-NP-a, (**b**) 4-NP-b, (**c**) MB, and (**d**) BPA.

Supplementary table 1 | Elemental analyses of all porous polymers. Fluorine contents were quantitatively measured by Combustion Ion Chromatography (CIC).

	Element	C	N	H	O	F
COP-99	Expected (%)	47.08	-	-	15.68	37.24
	Found (%)	50.05	0.92	0.87	26.73	21.51
F-CTF	Expected (%)	48.02	14.00	-	-	37.98
	Found (%)	60.16	21.26	2.82	-	15.82
CTF	Expected (%)	74.99	21.86	3.15	-	-
	Found (%)	67.49	17.93	2.38	6.7	-

Supplementary note 1. Long-term boiling test of COP-99 was carried out under hydrothermal condition. In order to prevent from the possible evaporation of D_2O under the elevated temperature, we carried out the test in closed glass ampoule. Typically, about 20 mg of COP-99 was placed in a Pyrex ampoule (5 mL capacity) and 1.5 mL of D_2O was transferred in the ampoule. The reaction mixture was frozen in liquid nitrogen, further evacuated and flame-sealed. After being warmed, the ampoule was treated at 110ºC for 24h, and the reaction filtrate was analysed using NMR spectroscopy.

We observed that COP-99 did not exhibit any colour change and the D_2O filtrate also stayed transparent after the hydrothermal treatment (Supplementary Fig. 2d). The ^{1}H NMR spectrum of the D_2O filtrate only showed a D_2O residual peak, and the ^{13}C NMR spectrum also displayed no peaks, indicating the COP-99 is insoluble in water even at a boiling condition (Supplementary Fig. 2e and 2f, respectively). In the ^{19}F NMR spectrum (Supplementary Fig. 2g), however, showed a small peak at about -130.27 ppm, corresponding to aqueous F^- ions (e.g. Aqueous F- of KF = -125.3 ppm). This implies that few fluorines on COP-99 were detached from the polymer network at the elevated temperature, and we assumed that D_2O replaces fluorines to produce deuterium fluoride in high temperature via nucleophilic substitution. When COP-99 was treated under lower temperature, i.e., 50 ºC for 60 h, there were no peaks in ^{1}H, ^{13}C, ^{19}F NMR spectrum in the D_2O filtrate (Supplementary Fig. 2h). We found that the fluorine content has been decreased 4.6 % after the boiling test at 110 ºC (only 20 % of all fluorines) due to the fluorine exchange with D_2O, however, there was no noticeable change in fluorine content after the treatment at 50 ºC. This indicates that the nucleophilic substitution of fluorines is plausible (albeit minor) under boiling condition, but the COP-99 was stable in water at least up to 50 ºC with no change in the amount of fluorines and its framework is stable even at high temperature and pressures. Therefore, COP-99 should be safe to be utilized in water treatment application owing to its stability and insolubility in water.

Supplementary note 2. The CO_2 and N_2 uptakes of the COP-99 were carried out at 273 K and 298 K (Supplementary Fig. 6a and 6b). The CO_2 isotherms of COP-99 show physisorptive binding motion with good reversibility. The CO_2 adsorption capacity of COP-99 at 1 bar is 2.14 mmol g^{-1} at 273 K and 1.55 mmol g^{-1} at 298 K, showing noticeable capacity retention with rising temperature. The CO_2 uptake of COP-99 under the high temperature is highly comparable to fluorinated porous polymers with much higher BET surface area, such as FPOP (2.2 mmol g^{-1} at 273 K, surface area = 1170 m^2 g^{-1})[5] and FMOP (1.68 mmol g^{-1} at 298 K, surface area = 1018 m^2 g^{-1})[6], which may be originated from the high fluorine content and narrower pore of COP-99 facilitating CO_2 adsorption[3, 7]. The preferential CO_2 binding capability of COP-99 was evaluated by using an ideal adsorbed solution theory (IAST) for binary mixture composition of CO_2:N_2 (15:85)[8]. The IAST CO_2 and N_2 selectivity was high as 29.6 at 273 K and 34.6 at 298 K, showing a slight enhancement in increasing temperature (Supplementary Fig. 6c). Such behaviour is due to CO_2 binding affinity toward the fluorinated COP-99 not weakening as much as the N_2 binding[9]. The isosteric heat (Q_{st}) of COP-99 for CO_2 adsorption was 21.3 kJ mol^{-1} at zero coverage (Supplementary Fig. 6d), indicating that COP-99 can be easily regenerated via pressure/vacuum swing adsorption technique.

Supplementary note 3. Along with 4-NP/BBG mixture shown in Fig. 7b, mixture of MB and BPA having similar molecular size was also tested for column separation and batch adsorption. When MB/BPA mixture was filtered through the COP-99 column, both molecules exhibited concentration decrease in a similar level, showing the removal efficiency of 47 % and 55.4 % for MB and BPA, respectively (Supplementary Fig. 16b). We believe this is originated from the column packing condition as we have seen the separation test result from 4-NP/BBG mixture. The size-dependent separation was dominant than the charge-based separation when the mixed molecules pass through a densely packed column, and MB and BPA having almost similar molecular size were filtered out at the same time. While there was no selective adsorption in the column separation, COP-99 showed charge-selective uptake of MB out of the MB/BPA dye mixture via batch adsorption. After immersing 8 mg of COP-99 in the 8 mL of MB/BPA mixed solution for 12 h, MB was removed up to 87 % and BPA was adsorbed 22 %, indicating the fluorine-charge interaction facilitates selective adsorption of MB from the mixed solution (Supplementary Fig. 16d).

Supplementary references

1. Budd PM*, et al.* Solution-processed, organophilic membrane derived from a polymer of intrinsic microporosity. *Adv. Mater.* **16**, 456-459 (2004).

2. Kuhn P, Antonietti M, Thomas A. Porous, covalent triazine-based frameworks prepared by ionothermal synthesis. *Angew. Chem. Int. Ed.* **47**, 3450-3453 (2008).

3. Zhao YF, Yao KX, Teng BY, Zhang T, Han Y. A perfluorinated covalent triazine-based framework for highly selective and water-tolerant CO_2 capture. *Energy Environ. Sci.* **6**, 3684-3692 (2013).

4. Clark T, Hennemann M, Murray J, Politzer P. Halogen bonding: the σ-hole. *J. Mol. Model.* **13**, 291-296 (2007).

5. Liu DP, Chen Q, Zhao YC, Zhang LM, Qi AD, Han BH. Fluorinated Porous Organic Polymers via Direct C-H Arylation Polycondensation. *ACS Macro Lett.* **2**, 522-526 (2013).

6. Yang ZZ*, et al.* Fluorinated microporous organic polymers: design and applications in CO_2 adsorption and conversion. *Chem. Commun.* **50**, 13910-13913 (2014).

7. Li GY, Zhang B, Yan J, Wang ZG. The directing effect of linking units on building microporous architecture in tetraphenyladmantane-based poly(Schiff base) networks. *Chem. Commun.* **50**, 1897-1899 (2014).

8. Myers AL, Prausnitz JM. Thermodynamics of mixed-gas adsorption. *AIChE J.* **11**, 121-127 (1965).

9. Patel HA, Ko D, Yavuz CT. Nanoporous Benzoxazole Networks by Silylated Monomers, Their Exceptional Thermal Stability, and Carbon Dioxide Capture Capacity. *Chem. Mater.* **26**, 6729-6733 (2014).

10. Baranowska I, Pieszko C, Raróg D, Pielesz A. Analysis of some aromatic amines by means of derivative spectrophotometry. *J. Environ. Sci. Heal. A* **37**, 1841-1848 (2002).